

## Electronic and Magnetic Properties of $RMO_3$ ( $M = Co, Fe$ ) Perovskites: a First Principle Study

V.M. Shved\*, V.M. Hreb, L.O. Vasylechko

Lviv Polytechnic National University, 12, S. Bandera St., 79013 Lviv, Ukraine

(Received 17 June 2019; revised manuscript received 23 October 2019; published online 25 October 2019)

The electronic structure and magnetic properties of orthorhombic  $PrFeO_3$  were evaluated by using GGA+U approach. It was found that AFM ordering is energetically favorable and more stable in the case of orthorhombic  $PrFeO_3$ . We also have performed a systematic investigation of the effect of the  $U$  parameter on the electronic structure of  $PrFeO_3$ . According to our calculations, the  $U$  correction for Fe  $3d$  should be of 6.8 eV and 7 eV for Pr  $4f$  to obtain the experimental band gap value.

The electronic structure calculations of orthorhombic  $PrCoO_3$  were performed by means of hybrid functional PBE0. The insulating and non-magnetic ground state of  $PrCoO_3$  was eventually obtained. Our calculations showed that the optimal amount of exact Hartree-Fock exchange (mixing parameter) of 0.14 is the most appropriate for treating  $PrCoO_3$ . The experimental values of lattice constants and atomic positions of  $PrCoO_3$  and  $PrFeO_3$  were used in all calculations.

**Keywords:** Electronic structure, Density of states, Magnetic moment, GGA+U, Hybrid functional.

DOI: [10.21272/jnep.11\(5\).05032](https://doi.org/10.21272/jnep.11(5).05032)

PACS numbers: 71.15.Ap, 71.20.Be

### 1. INTRODUCTION

In recent years, the perovskite-type oxides  $RMO_3$  (where R and M are rare earth and transition metals, respectively) have been extensively investigated due to their unique physical properties. In particular, rare-earth ferrites  $RFeO_3$  are known as canted antiferromagnets that possess magneto-optical and multiferroic properties as well as magnetization reversal, spin switching induced by temperature or magnetic field [1-6]. Rare-earth cobaltites  $RCoO_3$  exhibit magnetic and transport properties which can depend significantly on spin state transitions [7]. These oxides have been regarded as potential materials for photocatalysis, gas sensors and solid-oxide fuel cells [8-11].

The crystal structure of mixed praseodymium cobaltites-ferrites  $PrCo_{1-x}Fe_xO_3$  ( $0 \leq x \leq 1$ ) has been investigated by means of X-ray powder diffraction technique and synchrotron radiation sources [12, 13]. The orthorhombic perovskite-type structure with the space group of  $Pbnm$  (62) was observed in all samples. The obtained values of lattice constants and atomic positions for "pure"  $PrCoO_3$  and  $PrFeO_3$  were used in calculations of the electronic structure of these compounds.

Rare-earth cobaltites  $PrCoO_3$  and ferrites  $PrFeO_3$  are strongly correlated materials containing incomplete  $d$  and  $f$  shells. The description of the materials with strong electronic correlations is a great challenge for *ab initio* calculations for several reasons: the metallic state might be predicted for insulators, and the incorrect magnetic ordering could be obtained. The local density and general gradient approximations (LDA, GGA) are not able to describe qualitatively the electronic and magnetic properties of these materials [15, 18]. The limitations of LDA/GGA in treating localized partially filled  $d$  and  $f$  states can be overcome by applying hybrid functional or DFT+U scheme [16-18]. Both approaches depend on semi-empirical parameters such as mixing parameter in hybrid functional and effective Coulomb

interaction in DFT+U [19, 20].

In contrast to  $LaCoO_3$ , reported electronic structure calculations of  $PrCoO_3$  are limited [15, 21, 22]. Electronic states of  $PrCoO_3$  have been investigated by means of X-ray photoemission spectroscopy as well as LDA and LDA+U studies [15, 22]. Pandey et al. [15] pointed out that interactions between Pr  $4f$  electrons should be taken into account in  $PrCoO_3$  for better agreement with the experimental valence band spectrum. The insulating low-spin  $PrCoO_3$  was predicted within DFT+ $U_{sc}$  [21]. The GGA study of the electronic structure and magnetic properties of cubic  $PrFeO_3$  was performed recently and the metallic behavior was observed [14]. At the GGA+U level, cubic  $PrFeO_3$  was found to be a half-metallic [23]. But the electronic and magnetic properties of orthorhombic  $PrFeO_3$  perovskite have not been studied yet from the first principles, which is the most widely used type structure in technological applications.

In this work, we have studied systematically the influence of  $U$  correction on the band structure and magnetic properties of orthorhombic  $PrFeO_3$  by means of GGA+U method. Since the DFT+U investigations of orthorhombic  $PrCoO_3$  have already been reported, we have calculated the electronic structure of this material by means of hybrid functional PBE0. The optimal amount of Hartree-Fock exchange was determined to reach the reference band gap of  $PrCoO_3$ .

### 2. CALCULATION DETAILS

The ground state electronic structure was calculated using the projector augmented-wave method implemented in the ABINIT package [24, 25]. In this work, different approximations of DFT, such as GGA+U and PBE0 hybrid functional [19, 20], were employed to take into account the Coulomb repulsion between highly localized  $3d$  or  $4f$  electrons. Here, we have adopted the GGA+U scheme according to Dudarev et al. [19]. The effective Coulomb repulsion energy is treated as

\* [shvedvira@gmail.com](mailto:shvedvira@gmail.com)

$U_{eff} = U - J$ , where  $U$  and  $J$  are the Coulomb interaction and the exchange, respectively.

Exchange-correlation hybrid functional PBE0 is determined by the equation [20]:

$$E_{xc}^{PBE0}[n] = E_{xc}^{PBE}[n] + \alpha(E_x^{HF}[\Psi_{sel}] - E_x^{PBE}[n_{sel}]),$$

where  $E_x^{HF}$  and  $E_x^{PBE}$  are the Hartree-Fock and PBE exchange energy, respectively,  $E_c^{PBE}$  is the PBE correlation energy. PBE0 hybrid functional includes parameter  $\alpha$  which mixes the contribution of the Hartree-Fock and PBE exchange energy. There are two important parameters  $U_{eff}$  and  $\alpha$  that significantly affect the band structure.

We have adopted the energy cutoff of 545 eV in the wave function expansion. The valence basis sets for each atom were used as follows:  $5s^2 5p^6 6s^2 5d^1 4f^2$  for Pr,  $3s^2 3p^6 4s^1 3d^8$  for Co,  $3s^2 3p^6 4s^1 3d^7$  for Fe,  $2s^2 2p^4$  for O with the radii of the augmentation spheres of 2.5, 2.1, 2.1, 1.4 a.u., respectively. Integration over the Brillouin zone was performed on  $6 \times 6 \times 4$  Monkhorst-Pack  $k$  point mesh [26]. For GGA+U calculations, the full localized limit (FLL) double-counting method was chosen [27].

All calculations were performed using the experimental geometry. The experimental values of the lattice parameters of  $\text{PrCoO}_3$  and  $\text{PrFeO}_3$  were taken from [12]:  $a = 5.3754 \text{ \AA}$ ,  $b = 5.3392 \text{ \AA}$ ,  $c = 7.5741 \text{ \AA}$  and  $a = 5.48312 \text{ \AA}$ ,  $b = 5.57855 \text{ \AA}$ ,  $c = 7.78656 \text{ \AA}$ , respectively.

### 3. RESULTS AND DISCUSSION

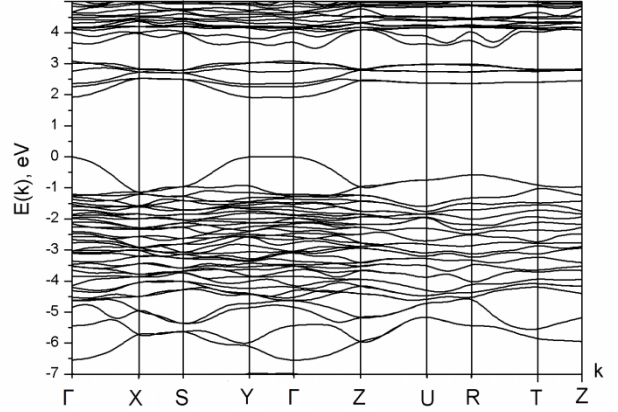
#### 3.1 Electronic Structure and Magnetic Properties of $\text{PrFeO}_3$

Initially, the electronic structure of orthorhombic  $\text{PrFeO}_3$  was calculated within GGA. But GGA incorrectly predicts a metallic ground state in  $\text{PrFeO}_3$  in contrast to the experimentally observed insulating character. This approximation fails for highly localized  $d/f$  states due to a self-interaction error. For more accurate description of the electronic structure and magnetic properties of  $\text{PrFeO}_3$ , the GGA+U approach was employed. The antiferromagnetic configuration (AFM) and ferromagnetic alignment (FM) were investigated in  $\text{PrFeO}_3$ . According to our total energy calculations, AFM ordering is energetically favorable with respect to the FM one which is consistent with experimental study [28]. Therefore, in this work we will consider only AFM phase as the most stable.

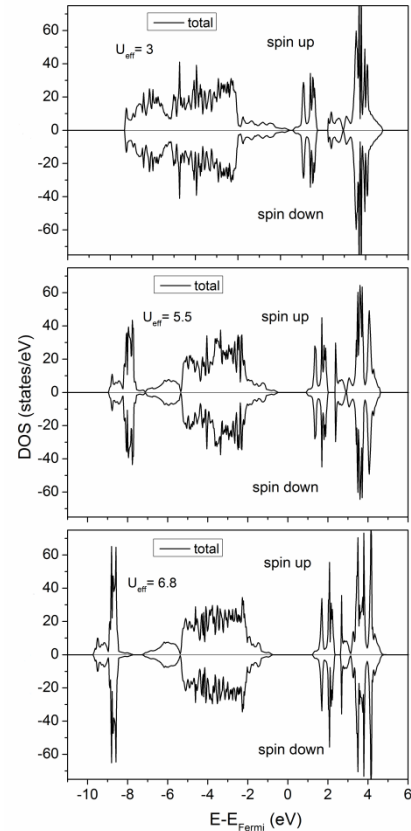
The localized Pr  $f$  electrons are treated with the effective Coulomb interaction ( $U_{eff}$ ) of 7 eV which is most commonly used in calculations [23, 29], while  $U_{eff}$  for Fe  $d$  electrons varies from 3 to 7 eV. In case of orthorhombic  $\text{PrFeO}_3$  the band gap depends strongly on  $U_{eff}$  for Fe. We have observed that at small  $U_{eff}$ , GGA+U also predicts the metallic state. These findings are in agreement with a more recent GGA+U study of cubic  $\text{PrFeO}_3$  [23].

The change in the value of the band gap and magnetic moment of  $\text{Fe}^{3+}$  ions with respect to  $U_{eff}$  is shown in Table 1. At around  $U_{eff} = 4$  eV,  $\text{PrFeO}_3$  becomes insulating but band gap of 0.60 eV is dramatically underestimated. In  $\text{PrFeO}_3$ , the experimentally observed gap is ranging between 1.88 and 2.08 eV [30, 31]. As  $U_{eff}$

changes from 4 to 7 eV, the gap increases almost linearly. When  $U_{eff} = 5.5$  eV, the experimental magnetic moment of  $\text{Fe}^{3+}$  is reproduced but the gap of 1.35 eV is still underestimated. An improved band gap of 1.78 eV was found by applying the  $U$  correction of 6.5 eV. As can be seen in Table 1, the local magnetic moment of  $\text{Fe}^{3+}$  is slightly overestimated for  $U$  values higher than 5.5 eV. To obtain the experimental band gap, the effective Coulomb interaction for Fe should be of about 6.8 eV and higher. For example, the suitable  $U_{eff}$  of 6.3 eV for Co and 7 eV for Pr were obtained from constrained DFT in  $\text{PrCoO}_3$  [32].



**Fig. 1** – Calculated band structure of  $\text{PrFeO}_3$  within GGA+U ( $U_{eff} = 6.8$  eV)

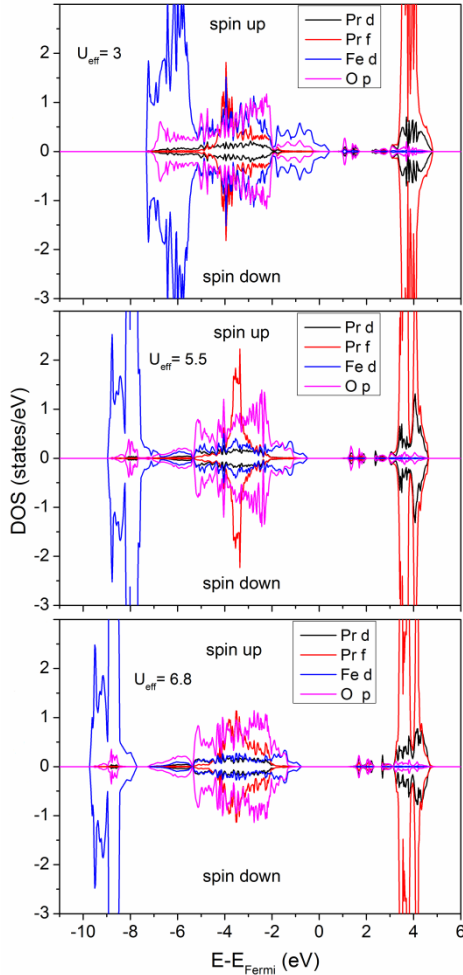


**Fig. 2** – Calculated total density of states of  $\text{PrFeO}_3$  using GGA+U with  $U_{eff}$ : 3, 5.5, 6.8 eV

**Table 1** – Calculated band gap and local magnetic moment of  $\text{Fe}^{3+}$  with different values of  $U_{\text{eff}}$  for Fe 3d ( $U_{\text{eff}}$  for Pr 4f is always equal to 7 eV)

	$U_{\text{eff}} = 3$ eV	$U_{\text{eff}} = 4$ eV	$U_{\text{eff}} = 5$ eV	$U_{\text{eff}} = 5.5$ eV	$U_{\text{eff}} = 6$ eV	$U_{\text{eff}} = 6.5$ eV	$U_{\text{eff}} = 6.8$ eV	$U_{\text{eff}} = 7$ eV	Exp.
$E_g$ , eV	–	0.60	1.13	1.35	1.64	1.78	1.92	2.07	1.88-2.08 [30, 31]
$M_{\text{Fe}}$ , $\mu_B$	3.78	3.97	4.09	4.14	4.19	4.22	4.25	4.26	4.14 [28]

The band structure of  $\text{PrFeO}_3$  with  $U_{\text{eff}}$  of 6.8 eV is presented in Fig. 1. Our calculations revealed that  $\text{PrFeO}_3$  is an indirect band gap material. The top of the valence band is located at  $\Gamma$  point and the bottom of the conduction band is at  $Y$  point. Fig. 2 and Fig. 3 illustrate the calculated total and partial densities of states of  $\text{PrFeO}_3$  with the following values of  $U_{\text{eff}}$ : 3.0, 5.5, and 6.8 eV. Fermi level is set to 0 eV. The densities of states are the same for two spin orientations, indicating on the antiferromagnetic ground state. Indeed, the total magnetic moment of the unit cell is equal to 0  $\mu_B$ .

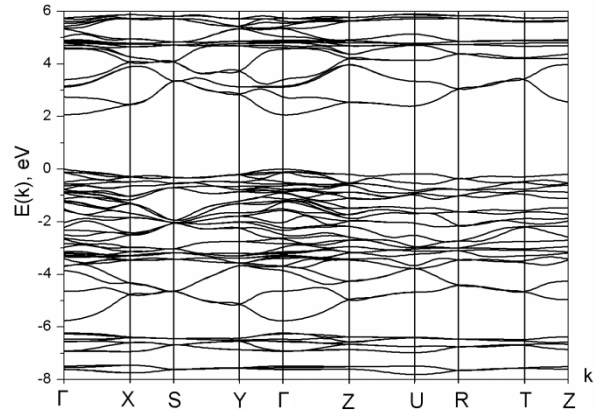
**Fig. 3** – Calculated partial density of states of  $\text{PrFeO}_3$  using GGA+U with  $U_{\text{eff}}$ : 3, 5.5, 6.8 eV

Increase in  $U_{\text{eff}}$  leads to the band gap opening in  $\text{PrFeO}_3$ , the lowest conduction band states move to higher energy. The shape and position of peaks of the valence band change when  $U$  varies from 5.5 eV to 6.8 eV. As  $U_{\text{eff}} = 6.8$  eV, the top of the valence band mainly consists of Fe  $d$  and O  $p$  states. The conduction band minimum is

composed predominantly of O  $p$  and Pr  $f, d$  states. With increasing  $U_{\text{eff}}$ , the valence band width is also increased. In the case of  $U_{\text{eff}} = 6.8$  eV, the valence band is separated into two bands. Fe  $d$  and O  $p$  states mostly contributed to the bottom of the valence band are pushed downward in energy. While the maximum peaks of unoccupied conduction band located at 3.22 and 4.64 eV remain almost unaffected. With increasing  $U_{\text{eff}}$ , the local magnetic moments of  $\text{Fe}^{3+}$  are increased from 3.78  $\mu_B$  ( $U_{\text{eff}} = 3.0$  eV) to 4.25  $\mu_B$  ( $U_{\text{eff}} = 6.8$  eV).

### 3.2 Electronic Structure of $\text{PrCoO}_3$

Since the electronic structure of  $\text{PrCoO}_3$  has already been studied within GGA+U [15, 21, 22], we will mainly focus on applying hybrid functional PBE0 in this work. At low temperatures  $\text{PrCoO}_3$  is a nonmagnetic insulator with  $\text{Co}^{3+}$  ions in the low spin (LS) configuration [7]. In this work,  $\text{PrCoO}_3$  is found to be a nonmagnetic at the ground state. The band gap significantly depends on the value of the mixing parameter  $\alpha$ . This parameter determines the amount of exact Hartree-Fock exchange and usually is set to 0.25 [20]. Recently it was shown that the band gap of  $\text{LaCoO}_3$  is significantly overestimated using the standard value of the mixing parameter [17]. Calculations based on HSE hybrid functional revealed that mixing parameter of 0.15 reproduces well the ground state properties of  $\text{LaMnO}_3$  [18]. So,  $\alpha$  may be system dependent.

**Fig. 4** – Calculated band structure of  $\text{PrCoO}_3$  using PBE0 ( $\alpha = 0.25$ )

We have performed the electronic structure calculations of  $\text{PrCoO}_3$  with different values of parameter  $\alpha$ , from 0.1 to 0.25. PBE0 with standard  $\alpha = 0.25$  predicts the band gap of 2.05 eV. The band dispersion of  $\text{PrCoO}_3$  is shown in Fig. 4.

The gap is direct, the valence band maximum and conduction band minimum are located at  $\Gamma$  point which

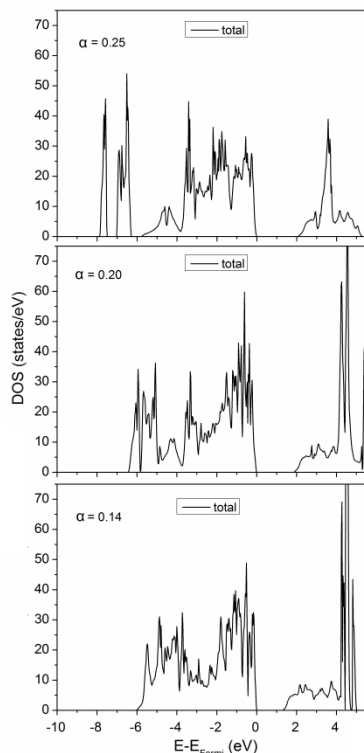


**Fig. 5** – Calculated total density of states of  $\text{PrCoO}_3$  using PBE0 with mixing parameter  $\alpha$ : 0.25, 0.2, 0.14

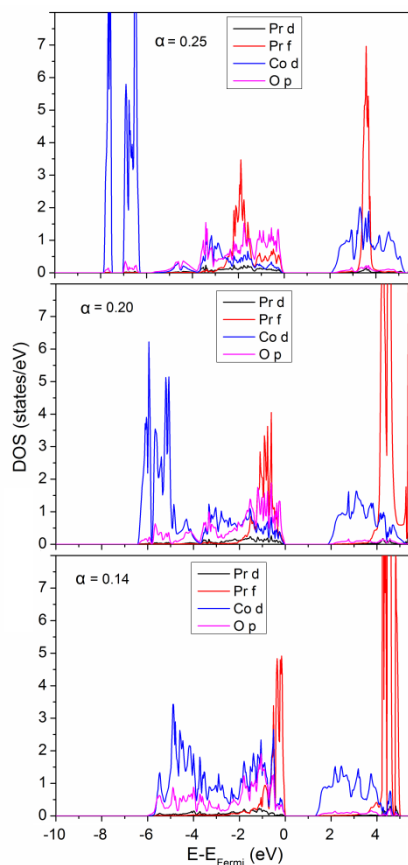


**Fig. 6** – Calculated partial density of states of  $\text{PrCoO}_3$  using PBE0 with mixing parameter  $\alpha$ : 0.25, 0.2, 0.14

is in agreement with the DFT+U study mentioned above [21]. Further, we consistently reduced the parameter  $\alpha$ , which is displayed in the total and partial densities of states (Fig. 5 and Fig. 6). As expected, the band gap is diminished when we reduce the amount of the Hartree-Fock exchange. The band gap decreases to 1.84 eV when  $\alpha = 0.2$ . For  $\alpha = 0.14$ , we have achieved a good agreement of gap value of 1.30 eV with reported GGA+U study and experimental data [21, 33]. The mixing parameter of 0.1 led to a narrower gap of 0.44 eV.

As can be seen in Fig. 6, when  $\alpha = 0.14$  the top of the valence band consists of O  $p$ , Pr  $f$ ,  $d$  and Co  $d$  states. The bottom of the conduction band is mainly formed by Co  $d$  states. The peaks of the valence band calculated with  $\alpha = 0.14$  are consistent with the experimental valence band spectrum [15]. As  $\alpha = 0.25$ , the valence band is characterized by three regions: the energy ranges of  $-7.84$ – $-7.52$  eV and  $-7.00$ – $-6.29$  eV are originated mainly from Co  $d$  states and the range of  $-5.81$  eV to the top of the valence band is mainly composed of Pr  $f$  states. The greater the amount of the Hartree-Fock exchange, the more delocalized the valence band. For larger values of the mixing parameter, Co  $d$  and Pr  $f$  states are shifted toward lower energy.

#### 4. CONCLUSIONS

In this work, the electronic structure of orthorhombic  $\text{PrCoO}_3$  and  $\text{PrFeO}_3$  perovskites was calculated using the experimental values of the lattice constants and atomic positions. The hybrid PBE0 predicts the correct nonmagnetic ground state in  $\text{PrCoO}_3$ . According to GGA+U study, the AFM phase is more favored over the FM in  $\text{PrFeO}_3$ , which is in a good agreement with the experimental data.

The calculated electronic structure indicates that orthorhombic  $\text{PrFeO}_3$  is indirect band gap material. It was shown in GGA+U study the influence of the  $U_{\text{eff}}$  on the value of the band gap and local magnetic moment of  $\text{Fe}^{3+}$  ions. For small values of  $U_{\text{eff}}$  for Fe  $3d$ ,  $\text{PrFeO}_3$  exhibits a metallic behavior. But with further increase of  $U_{\text{eff}}$ , the band gap changes almost linearly and reaches the experimental value at about  $U_{\text{eff}} = 6.8$  eV for Fe  $3d$  and  $U_{\text{eff}} = 7$  eV for Pr  $4f$ . In this case, the magnetic moment per  $\text{Fe}^{3+}$  ions increases gradually as a function of  $U_{\text{eff}}$ . For larger  $U_{\text{eff}}$  for Fe  $3d$  ( $U_{\text{eff}} > 5.5$  eV), GGA+U insignificantly overestimates the magnetic moment of  $\text{Fe}^{3+}$ . With increasing  $U_{\text{eff}}$  for Fe  $3d$ , the valence band width is also increased.

In the case of  $\text{PrCoO}_3$ , the change in the band gap value on the amount of the Hartree-Fock exchange (mixing parameter) was investigated. The direct band gap was predicted in  $\text{PrCoO}_3$ . The gap obtained with a mixing parameter of 0.14 is in close agreement with the experimental measurements. For larger mixing parameters the valence band is more extended.

#### ACKNOWLEDGEMENTS

The work was funded by the Ministry of Education and Science of Ukraine under project N 0118U000264 (DB/Feryt).

## REFERENCES

1. Y.S. Didosyan, H. Hauser, J. Nicolics, *Sens. Actuat.* **81**, 263 (2000).
2. Y. Tokunaga, S. Iguchi, T. Arima, Y. Tokura, *Phys. Rev. Lett.* **101**, 097205 (2008).
3. S.J. Yuan, W. Ren, F. Hong, Y.B. Wang, J.C. Zhang, L. Bellaiche, S.X. Cao, G. Cao, *Phys. Rev. B* **87**, 184405 (2013).
4. H. Shen, Z.X. Cheng, F. Hong, J.Y. Xu, S.J. Yuan, S.X. Cao, X.L. Wang, *Appl. Phys. Lett.* **103**, 192404 (2013).
5. J.H. Lee et al., *Phys. Rev. Lett.* **107**, 117201 (2011).
6. Y.K. Jeong, J.H. Lee, S.J. Ahn, H.M. Jang, *Solid State Commun.* **152**, 1112 (2012).
7. B. Raveau, Md. Motin Seikh, *Handbook of Magnetic Materials*, (Elsevier B.V. P.: 2015).
8. C. Tealdi, M.S. Islam, C.A.J. Fisher, L. Malavasi, G. Flor, *Prog. Solid State Chem.* **35**, 491 (2007).
9. J.W. Fergus, *Sens. Actuat.* **123**, 1169 (2007).
10. C. Sun, R. Hui, J. Roller, *J. Solid State Electrochem.* **14**, 125 (2010).
11. K.M. Parida, K.H. Reddy, S. Martha, D.P. Das, N. Biswal, *Int. J. Hydrogen Energy* **35**, 2161 (2010).
12. O.V. Kharko, L.O. Vasylechko, *Visnyk of Lviv Polytechnic National University* **734**, 34 (2012).
13. O. Pekinchak, L. Vasylechko, I. Lutsyuk, Ya. Vakhula, Yu. Prots, W. Carrillo-Cabrera, *Nanoscale Res. Lett.* **11**, 75 (2016).
14. K.E. Babu, V.V. Kumar, K.B. Kumari, K. Neeraja, N.G. Praveena, V. Veeraiah, *AIP Conf. Proc.* **1992**, 040036 (2018).
15. S.K. Pandey, A. Kumar, S.M. Chaudhari, A.V. Pimpale, *J. Phys.: Condens. Matter.* **18**, 1313 (2006).
16. T. Jia, Z. Zeng, H.Q. Lin, Y. Duan, P. Ohodnicki, *RSC Adv.* **7**, 38798 (2017).
17. X. Zhang, G. Fu, H. Wan, *Chin. J. Chem. Phys.* **27**, 274 (2014).
18. P. Rivero, V. Meunier, W. Shelton, *Phys. Rev. B* **93**, 024111 (2016).
19. S.L. Dudarev, G.A. Botton, S.Y. Savrasov, C.J. Humphreys, A.P. Sutton, *Phys. Rev. B: Condens. Matter. Mater. Phys.* **57**, 1505 (1998).
20. E. Tran, P. Blaha, K. Schwarz, P. Novak, *Phys. Rev. B* **74**, 155108 (2006).
21. M. Topsakal, C. Leighton, R.M. Wentzcovitch, *J. Appl. Phys.* **119**, 244310 (2016).
22. S.K. Pandey, A. Kumar, S. Banik, A.K. Shukla, S.R. Barman, A.V. Pimpale, *Phys. Rev. B* **77**, 113104 (2008).
23. M. Rezaiguia, W. Benstaali, A. Abbad, S. Bentata, B. Bouhaf, *J. Supercond. Nov. Magn.* **30**, 2581 (2017).
24. P.E. Blöchl, *Phys. Rev. B* **50**, 17953 (1994).
25. X. Gonze, B. Amadon, P.-M. Anglade, J.-M. Beuken, F. Bottin, P. Boulanger, F. Bruneval, D. Caliste, R. Caracas, M. Côté, T. Deutsch, L. Genovese, Ph. Ghosez, M. Giantomassi, S. Goedecker, D.R. Hamann, P. Hermet, F. Jollet, G. Jomard, S. Leroux, M. Mancini, S. Mazevet, M.J.T. Oliveira, G. Onida, Y. Pouillon, T. Rangel, G.M. Rignanese, D. Sangalli, R. Shaltaf, M. Torrent, M.J. Verstraete, G. Zerah, J.W. Zwanziger, *Comput. Phys. Commun.* **180**, 2582 (2009).
26. H.J. Monkhorst, J.D. Pack, *Phys. Rev. B* **13**, 5188 (1976).
27. A.I. Liechtenstein, V.I. Anisimov, J. Zaanen, *Phys. Rev. B* **52**, R5467 (1995).
28. I. Sosnowska, P. Fischer, *J. Less Common Met.* **111**, 109 (1985).
29. M. Chakraborty, P. Pal, B.R. Sekhar, *Solid State Commun.* **145**, 197 (2008).
30. C. Qin, Z. Li, G. Chen, Y. Zhao, T. Lin, *J. Power Sources* **285**, 178 (2015).
31. S.N. Tijare, S. Bakardjieva, J. Subrt, M.V. Joshi, S.S. Rayalu, S. Hishita, N. Labhsetwar, *J. Chem. Sci.* **126**, 517 (2014).
32. P. Dutta, S. Lal, S.K. Pandey, *AIP Conf. Proc.* **1942**, 090017 (2018).
33. S. Yamaguchi, Y. Okimoto, and Y. Tokura *Phys. Rev. B* **54**, 54 (1996).

### Електронні та магнітні властивості перовскітів $\text{RMO}_3$ ( $M = \text{Co}, \text{Fe}$ ): дослідження з перших принципів

В.М. Швед, В.М. Греб, Л.О. Василечко

Національний університет "Львівська політехніка", вул. С. Бандери, 12, 79013 Львів, Україна

Електронну структуру та магнітні властивості орторомбічного  $\text{PrFeO}_3$  оцінювали за допомогою підходу GGA+U. Було встановлено, що AFM впорядкування є енергетично вигіднішим та стабільнішим у випадку орторомбічного  $\text{PrFeO}_3$ . Ми також провели систематичне дослідження впливу параметра  $U$  на електронну структуру  $\text{PrFeO}_3$ . Згідно з нашими підрахунками, поправка  $U$  для  $\text{Fe } 3d$  повинна складати 6,8 eV і 7 eV для  $\text{Pr } 4f$ , щоб отримати експериментальне значення забороненої зони.

Розрахунки електронної структури орторомбічного  $\text{PrCoO}_3$  виконували за допомогою гібридного функціоналу PBE0. Зрештою було отримано ізоляційний та немагнітний основний стан  $\text{PrCoO}_3$ . Наші розрахунки показали, що оптимальна кількість точної обмінної енергії Хартрі-Фока (параметр змішування) 0,14 є найбільш підходящим для розгляду  $\text{PrCoO}_3$ . Експериментальні значення сталих решітки та положень атомів  $\text{PrCoO}_3$  та  $\text{PrFeO}_3$  використовувались у всіх розрахунках.

**Ключові слова:** Електронна структура, Щільність станів, Магнітний момент, GGA+U, Гібридний функціонал.